

Linda Arnfors,^a Thomas Hansen,^b
Winfried Meining,^a Peter
Schönheit^b and Rudolf
Ladenstein^{a*}

^aCenter for Structural Biochemistry, Department of Biosciences at Novum, Karolinska Institute, S-141 57 Huddinge, Sweden, and ^bInstitut für Allgemeine Mikrobiologie, Christian-Albrecht-Universität Kiel, 24118 Kiel, Germany

Correspondence e-mail:
rudolf.ladenstein@biosci.ki.se

Received 28 April 2005
Accepted 17 May 2005
Online 1 June 2005

Expression, purification, crystallization and preliminary X-ray analysis of a nucleoside kinase from the hyperthermophile *Methanocaldococcus jannaschii*

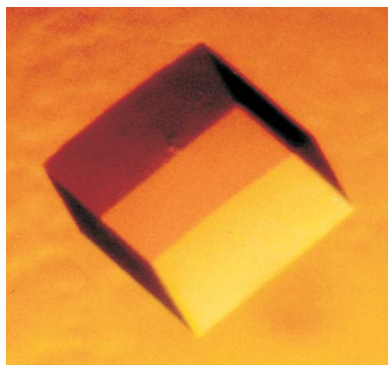
Methanocaldococcus jannaschii nucleoside kinase (*Mj*NK) is an ATP-dependent non-allosteric phosphotransferase that shows high catalytic activity for guanosine, inosine and cytidine. *Mj*NK is a member of the phosphofructokinase B family, but participates in the biosynthesis of nucleoside monophosphates rather than in glycolysis. *Mj*NK was crystallized as the apoenzyme as well as in complex with an ATP analogue and Mg²⁺. The latter crystal form was also soaked with fructose-6-phosphate. Synchrotron-radiation data were collected to 1.70 Å for the apoenzyme crystals and 1.93 Å for the complex crystals. All crystals exhibit orthorhombic symmetry; however, the apoenzyme crystals contain one monomer per asymmetric unit whereas the complex crystals contain a dimer.

1. Introduction

The phosphofructokinase B family (PFK-B family; Prosite PS00583 and PS00584; Pfam PF00294) is a diverse protein family within the ribokinase superfamily (SCOP 53613) present in all three domains of life: archaea, bacteria and eukarya. The PFK-B protein family includes a variety of non-allosteric ATP-dependent kinases, e.g. inosine-guanosine kinases, tagatose-6-phosphate kinases, ribokinases, fructokinases and 1-phosphofructokinases, as well as the minor 6-phosphofructokinase (PFK-B) from *Escherichia coli* and the 6-phosphofructokinases from the archaea *Desulfurococcus amylolyticus* and *Aeropyrum pernix* (Bork *et al.*, 1993; Hansen & Schönheit, 2000, 2001). The latter PFKs are not related to the ATP-dependent 6-phosphofructokinases from the phosphofructokinase A family (Pfam PF00365; Wu *et al.*, 1991; Ronimus & Morgan, 2001), which represent key regulatory enzymes in the Embden–Meyerhof pathways of various bacteria and eukarya (Wu *et al.*, 1991; Ronimus & Morgan, 2001; Hansen *et al.*, 2002). Moreover, ADP-dependent 6-phosphofructokinases and glucokinases constitute a separate protein family within the ribokinase superfamily (Pfam PF04587; Ito *et al.*, 2001).

Seven structures of enzymes from the PFK-B family have been described so far. These include *E. coli* ribokinase (PDB code 1rkd), human and *Toxoplasma gondii* adenosine kinases (1bx4 and 1dgm), the 2-keto-3-deoxygluconate kinases from *Thermotoga maritima* (1j5v) and *Thermus thermophilus* (1v1s), sheep pyridoxal kinase (1lhp) and putative 1-phosphofructokinase from *Thermotoga maritima* (1o14) (Sigrell *et al.*, 1998; Mathews *et al.*, 1998; Schumacher *et al.*, 2000; Ohshima *et al.*, 2004; Li *et al.*, 2002; Joint Center For Structural Genomics, unpublished results). A structure of an archaeal member of the PFK-B family has not yet been reported. The structures of the ADP-dependent glucokinases from *Thermococcus litoralis* (PDB code 1gc5) and *Pyrococcus furiosus* (1ua4) were the first archaeal representatives within the ribokinase superfamily (Ito *et al.*, 2001). For a better understanding of the evolution of the ribokinase superfamily as well as of sugar kinases in general, additional structures of members of the PFK-B family are necessary.

In 1996, when the complete genome of *Methanocaldococcus jannaschii* was released, Bult and coworkers described the gene product of MJ0406 as a hypothetical PFK-B sugar kinase (Bult *et al.*,



© 2005 International Union of Crystallography
All rights reserved

1996). Owing to sequence similarity to the *A. pernix* PFK-B 6-phosphofructokinase (Hansen & Schönheit, 2001), it has been suggested that MJ0406 might also encode a PFK-B. However, characterization of the respective heterologous protein revealed that MJ0406 catalyzes the ATP-dependent phosphorylation of several substrates. The enzyme, which was designed as a nucleoside kinase (*Mj*NK), showed the highest catalytic activity with guanosine, inosine and cytidine, but used fructose-6-phosphate only to a very low extent (Hansen & Schönheit, unpublished work). Thus, *Mj*NK plays a role in the nucleoside metabolism rather than in sugar degradation in *M. jannaschii*.

Moreover, the three-dimensional structure of *Mj*NK will help in understanding the wide substrate range of the enzyme as well as the evolution and non-allosteric nature of the PFK-B family and will provide additional data on the structural factors that give rise to thermostability of proteins.

Here, we describe the expression, purification, crystallization and preliminary X-ray analysis of *M. jannaschii* nucleoside kinase.

2. Materials and methods

2.1. Expression

E. coli BL 21 (DE3) pLys S cells were transformed with a pET-17b plasmid which contained the *mjnk* gene (Hansen & Schönheit, unpublished work). Transformed cells were grown in 400 ml Luria-Bertani medium with 100 µg ml⁻¹ carbenicillin and 34 µg ml⁻¹ chloramphenicol at 310 K. When the cells reached an optical density at 600 nm of 0.8, protein expression was induced by the addition of 0.8 mM IPTG. After further 4 h of growth (OD₆₀₀ ≈ 3.2–3.6), the cells were harvested by centrifugation at 277 K and then washed in a buffer containing 50 mM Tris–HCl pH 7.0 and 50 mM NaCl.

2.2. Purification

All chromatographic steps were carried out at 277 K. Cell extracts were prepared by French press treatment (1.3 × 10⁸ Pa) of cell suspensions in buffer *A* (50 mM Tris–HCl pH 8.4). After ultracentrifugation (100 000g for 60 min), the solution was heat-precipitated at 353 K for 45 min, centrifuged again (15 000g for 30 min), dialyzed three times against a 30-fold excess of 50 mM Tris–HCl pH 8.0 (buffer *B*) and applied onto a DEAE Sepharose column (60 ml) previously equilibrated with buffer *B*. The protein was eluted at a flow rate of 3 ml min⁻¹ with 180 ml 50 mM piperazine pH 6.5 at 298 K (buffer *C*) as well with a combination of fixed NaCl concentration and linear gradients from 0 to 2 M NaCl in buffer *B*: 0–0.1 M (120 ml), 0.1–1 M (180 ml), 1–2 M (120 ml) and 2 M NaCl (120 ml). Fractions containing the highest nucleoside kinase activity (160 ml, 0.2–1 M NaCl) were pooled and diluted with 3 M ammonium sulfate in buffer *B* to a final ammonium sulfate concentration of 2 M. Subsequently, the solution was applied onto a phenyl-Sepharose column (15 ml) previously equilibrated with 2 M ammonium sulfate in buffer *B*. The protein was eluted with a linear ammonium sulfate gradient (2–0 M, 150 ml) followed by washing the column with 60 ml 50 mM Tris–HCl pH 8.0 and 60 ml water. Fractions containing nucleoside kinase activity (75 ml, 1.2–0.2 M ammonium sulfate) were checked for purity with respect to protein and DNA impurities. *Mj*NK, which was almost pure (45 ml, 0.8–0.2 M ammonium sulfate, protein and DNA contamination <5%), was used for further purification. The protein was concentrated by ultrafiltration (exclusion size 10 kDa) and then applied onto a Superdex 200 gel-filtration column (120 ml) previously equilibrated with buffer *D* (150 mM NaCl,

50 mM Tris–HCl pH 7.5); pure *Mj*NK was obtained (72–86 ml) from this step.

2.3. Crystallization

M. jannaschii nucleoside kinase was dialyzed against 20 mM Tris–HCl pH 8.0 containing 0.02% sodium azide, concentrated to a protein concentration of 13 mg ml⁻¹ and kept at 277 K. For crystallization of the complex, *Mj*NK was mixed with the ATP analogue AMPPNP and MgCl₂ in the ratio 1:10:20 and incubated for at least 15 h. In order to find crystallization conditions for both the apo form (*Mj*NK-apo) and the complex with AMPPNP (*Mj*NK-A), homemade screening sets identical to commercially available screens [Crystal Screen I (Jancarik & Kim, 1991), Crystal Screen Lite (Jancarik & Kim, 1991; McPherson, 1990), Natrix (Scott *et al.*, 1995) and PEG/Ion Screen from Hampton Research] were used. Promising conditions were optimized using a finer grid search. All crystallization experiments were carried out at 293 K using the sitting-drop or hanging-drop vapour-diffusion methods; the latter method was preferred in order to prevent crystals from sticking to the plate. 2.5 µl mother liquor was added to a fresh drop of an equal volume of protein solution and the drops were allowed to equilibrate against 500 µl mother liquor. A total concentration of 0.02% azide was used in all crystallization drops. Some of the complex crystals were further soaked with 10 mM

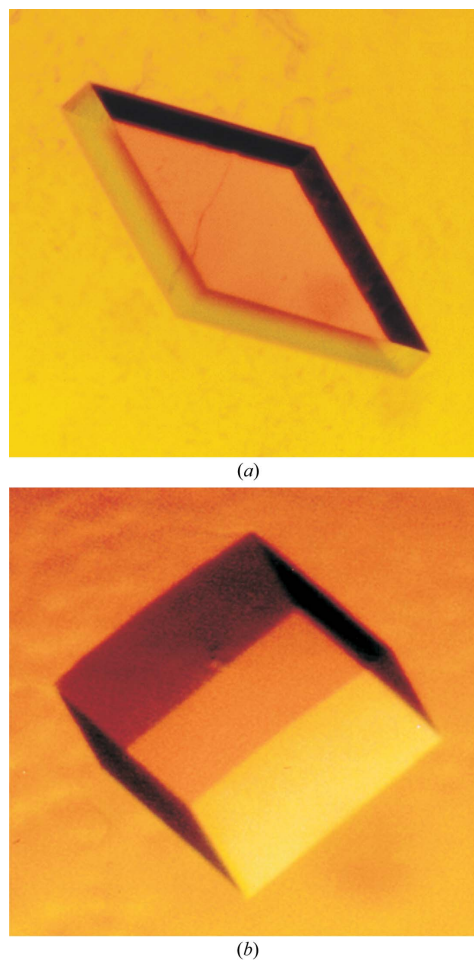


Figure 1 Orthorhombic crystals of *M. jannaschii* nucleoside kinase showing (a) the apo form (*Mj*NK-apo) and (b) the enzyme in complex with the ATP analogue AMPPNP and MgCl₂. The crystal sizes for *Mj*NK-apo and *Mj*NK-A were 0.1 × 0.3 × 0.3 and 0.2 × 0.2 × 0.2 mm, respectively.

Table 1
Crystallographic data analysis.

Values in parentheses are for the highest resolution shell.

	<i>Mj</i> NK-apo	<i>Mj</i> NK-A	<i>Mj</i> NK-AF
Space group	$P2_12_12$	$P2_12_12_1$	$P2_12_12_1$
Unit-cell parameters (Å, °)	$a = 64.1, b = 148.1, c = 41.1,$ $\alpha = \beta = \gamma = 90$	$a = 64.2, b = 83.2, c = 147.0,$ $\alpha = \beta = \gamma = 90$	$a = 64.0, b = 83.1, c = 146.8,$ $\alpha = \beta = \gamma = 90$
Resolution (Å)	50–1.70 (1.73–1.70)	20–1.93 (1.96–1.93)	20–1.93 (1.96–1.93)
No. of observations	694623	1132735	800362
Unique reflections	44110	58677	58526
Completeness (%)	100 (100)	97.4 (83.5)	97.0 (85.8)
$\langle I \rangle / \langle \sigma(I) \rangle$	41.5 (3.3)	19.3 (1.2)	19.9 (1.4)
R_{merge}^\dagger (%)	4.3 (65.4)	5.9 (55.7)	6.0 (65.7)
Subunits per AU	1	2	2
V_M (Å ³ Da ⁻¹)	2.88	2.90	2.88

$$\dagger R_{\text{merge}} = \sum |I - \langle I \rangle| / \sum I.$$

fructose-6-phosphate in mother liquor for at least 24 h. The soaked crystals are referred to as *Mj*NK-AF. Suitable cryoconditions were screened by the addition of polyethylene glycol 400, glycerol and ethylene glycol. The cryoprotectant solutions for each crystal form contained the mother-liquor composition with the addition of 30% ethylene glycol for *Mj*NK-apo and 20% ethylene glycol for *Mj*NK-A and *Mj*NK-AF.

2.4. Data collection and preliminary X-ray analysis

Prior to data collection, the crystals were soaked for 1 min in the cryoprotectant solution and flash-cooled in liquid nitrogen. Synchrotron-radiation data for *Mj*NK-apo were collected on beamline I711 at MAX-lab (Lund, Sweden) at a wavelength of 1.134 Å using a MAR Research imaging-plate detector. Data for the two complex forms were collected at beamline X11 at the EMBL Outstation, DESY (Hamburg, Germany) at a wavelength of 0.8098 Å using a MAR CCD detector. For all three crystal forms, both high-

and low-resolution data sets were collected. The data were indexed and scaled using the *HKL* package programs *DENZO* and *SCALEPACK* (Otwinowski & Minor, 1997).

3. Results and discussion

M. jannaschii nucleoside kinase has been crystallized in two forms: an apo form (*Mj*NK-apo) and a form with the protein in complex with AMPPNP and MgCl₂ (*Mj*NK-A). Some of the *Mj*NK-A crystals were further soaked with fructose-6-phosphate (*Mj*NK-AF).

*Mj*NK-apo crystals were obtained from a solution containing 10% (w/v) PEG 3500 and 0.15 M magnesium acetate. *Mj*NK-A crystallized from a solution containing 15% PEG 4000, 0.10 M MgCl₂ and 0.1 M Tris-HCl pH 8.5. Colourless orthorhombic crystals (Fig. 1) appeared within 1–4 d.

Data-collection parameters and statistics of the three crystal forms of *M. jannaschii* nucleoside kinase are summarized in Table 1. Pseudo-precession photographs (Lu, 1999) of the diffraction data evaluated in space group *P222* showed systematic extinctions at $h = 2n + 1, k = 2n + 1, l = 2n$ for *Mj*NK-apo and $h = 2n + 1, k = 2n + 1, l = 2n + 1$ for *Mj*NK-A and *Mj*NK-AF. The space groups were thus assigned as $P2_12_12$ for *Mj*NK-apo and $P2_12_12_1$ for the two complex forms. Moreover, the unit-cell parameters of the apo form and the complexes are almost identical with one exception. The *b* axes of the complexes ($b = 83.2$ Å for *Mj*NK-A and $b = 83.1$ Å for *Mj*NK-AF) are twice as long as the *c* axis for *Mj*NK-apo ($c = 41.1$ Å). This results in a unit-cell volume twice the size for the complex crystals and thus the unit cell of *Mj*NK-apo contains half the number of subunits compared with *Mj*NK-A and *Mj*NK-AF. In addition, the calculated Matthews coefficient (V_M ; Matthews, 1968) of 2.88 Å³ Da⁻¹ for four monomers in the unit cell of *Mj*NK-apo indicated that the crystal contains one subunit per asymmetric unit. This corresponds to a solvent content of 56.9%. Gel-filtration data reveals that *Mj*NK exists as a dimer in solution (Hansen & Schönheit, unpublished results). Therefore, it is concluded that the biological dimer is generated by a twofold crystallographic symmetry operation in the apo crystals. Owing to the different unit-cell volumes and according to the calculated Matthews coefficients (Table 1), *Mj*NK-A and *Mj*NK-AF contain one dimer per asymmetric unit, with solvent contents of 57.2 and 56.9%, respectively. The self-rotation function obtained from the *Mj*NK-A and *Mj*NK-AF data, calculated with the programs *MOLREP* (Vagin & Teplyakov, 1997), *AMoRe* (Navaza, 1994) and *POLARRFN* (Collaborative Computational Project, Number 4, 1994) in the *CCP4* suite, shows no additional twofold symmetry apart from crystallographic symmetry (Fig. 2). Furthermore, the native Patterson map calculated with *FFT* (Read & Schierbeek, 1988) within

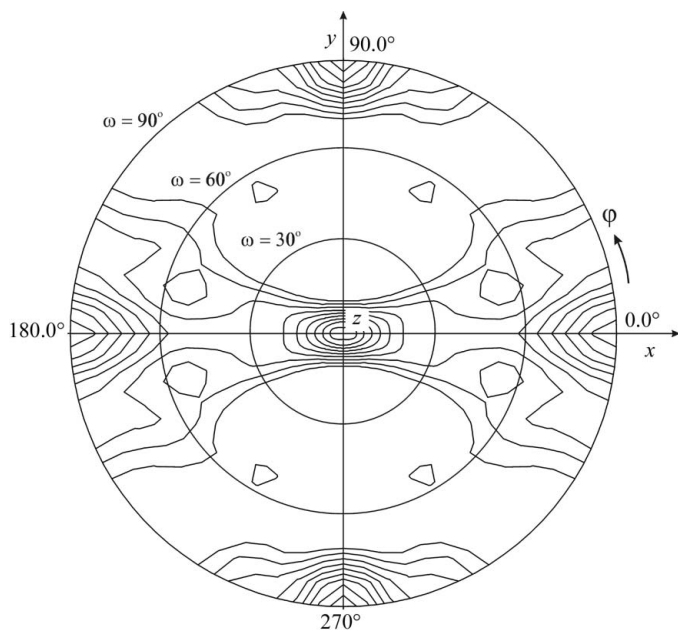


Figure 2
Stereographic plot of the self-rotation function at the section $\kappa = 180^\circ$ calculated from the *Mj*NK-AF data. The integration radius is between 15 and 5 Å and the resolution limits are 10–4 Å. Contour lines are drawn in steps of 10%. Only high peaks arising from crystallographic symmetry can be seen, which indicates that the twofold non-crystallographic axis is parallel to a crystallographic axis. The plot was produced using *POLARRFN* (Collaborative Computational Project, Number 4, 1994).

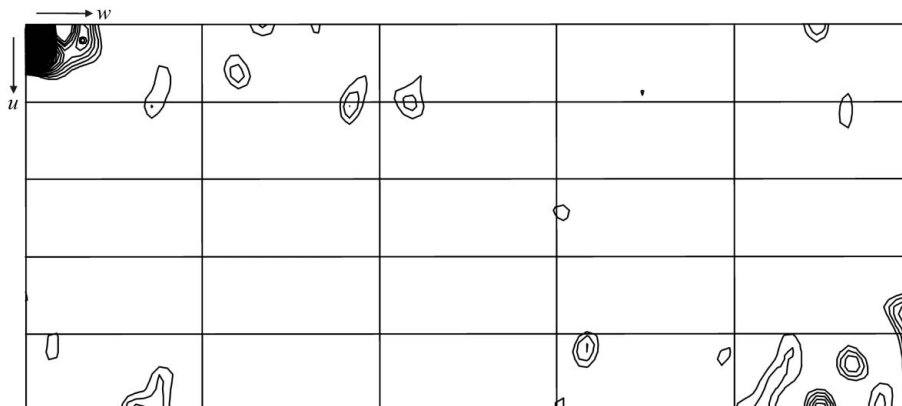


Figure 3 Native Patterson function calculated from all data from the MjNK-AF complex. The plot shows fractional coordinates of u and w ranging from 0.0 to 0.5 at Harker section $v = 0.5$. An intense pseudo-origin peak appears at $(u, w) = (0.0, 0.0)$. Grid lines are drawn every 0.10 units and contours are drawn every 0.5% of the origin peak height, starting at 1.5%. The figure was prepared with the programs *NPO* and *PLTDEV* from the *CCP4* suite (Collaborative Computational Project, Number 4, 1994).

the *CCP4* suite of programs reveals a pseudo-origin peak at $(u, v, w) = (0.0, 0.5, 0.0)$ (Fig. 3) with an intensity of 25% of the Patterson origin peak. The results from the self-rotation function and the native Patterson indicate that the twofold non-crystallographic symmetry axis relating the two subunits in the asymmetric unit is parallel to the y axis in the unit cell.

We gratefully acknowledge MAX-lab (Lund, Sweden) and the EMBL Outstation at DESY (Hamburg, Germany) for provision of synchrotron-radiation facilities. We thank the European Community Research Infrastructure Action under the FP6 'Structuring the European Research Area Programme' contract No. HPRI/1999/CT/00017 for travel expenses and NorFA (Norway) for financial support under the 'Biology of Thermophiles' project.

References

- Bork, P., Sander, C. & Valencia, A. (1993). *Protein Sci.* **2**, 31–40.
 Bult, C. J. *et al.* (1996). *Science*, **273**, 1058–1073.
 Collaborative Computational Project, Number 4 (1994). *Acta Cryst.* **D50**, 760–763.
 Hansen, T., Musfeldt, M. & Schönheit, P. (2002). *Arch. Microbiol.* **177**, 401–409.
 Hansen, T. & Schönheit, P. (2000). *Arch. Microbiol.* **173**, 103–109.
 Hansen, T. & Schönheit, P. (2001). *Arch. Microbiol.* **177**, 62–69.
 Ito, S., Fushinobu, S., Yoshioka, I., Koga, S., Matsuzawa, H. & Wakagi, T. (2001). *Structure*, **9**, 205–214.
 Jancarik, J. & Kim, S.-H. (1991). *J. Appl. Cryst.* **24**, 409–411.
 Li, M. H., Kwok, F., Chang, W. R., Lau, C. K., Zhang, J. P., Lo, S. C., Jiang, T. & Liang, D. C. (2002). *J. Biol. Chem.* **277**, 46385–46390.
 Lu, G. (1999). *J. Appl. Cryst.* **32**, 375–376.
 McPherson, A. (1990). *Eur. J. Biochem.* **189**, 1–23.
 Mathews, I. I., Erion, M. D. & Ealick, S. E. (1998). *Biochemistry*, **37**, 15607–15620.
 Matthews, B. W. (1968). *J. Mol. Biol.* **33**, 491–497.
 Navaza, J. (1994). *Acta Cryst.* **A50**, 157–163.
 Ohshima, N., Inagaki, E., Yasuike, K., Takio, K. & Tahirov, T. (2004). *J. Mol. Biol.* **340**, 477–489.
 Otwinowski, Z. & Minor, W. (1997). *Methods Enzymol.* **276**, 307–326.
 Read, R. J. & Schierbeek, A. J. (1988). *J. Appl. Cryst.* **21**, 490–495.
 Ronimus, R. S. & Morgan, H. W. (2001). *Extremophiles*, **5**, 357–373.
 Schumacher, M. A., Scott, D. M., Mathews, I. I., Ealick, S. E., Roos, D. S., Ullman, B. & Brennan, R. G. (2000). *J. Mol. Biol.* **298**, 875–893.
 Scott, W. G., Finch, J. T., Grenfell, R., Fogg, J., Smith, T., Gait, M. J. & Klug, A. (1995). *J. Mol. Biol.* **250**, 327–332.
 Sigrell, J. A., Cameron, A. D., Jones, T. A. & Mowbray, S. L. (1998). *Structure*, **6**, 183–193.
 Vagin, A. & Teplyakov, A. (1997). *J. Appl. Cryst.* **30**, 1022–1025.
 Wu, L.-F., Reizer, A., Reizer, J., Cai, B., Tomich, J. M. & Saier, M. H. Jr (1991). *J. Bacteriol.* **173**, 3117–3127.